International Journal of Thermal Sciences 87 (2015) 103–109

Contents lists available at ScienceDirect

International Journal of Thermal Sciences

journal homepage: www.elsevier.com/locate/ijts

An explicit analytical model for rapid computation of temperature field in a three-dimensional integrated circuit (3D IC)

Leila Choobineh, Ankur Jain*

Mechanical and Aerospace Engineering Department, University of Texas at Arlington, Arlington, TX, USA

ARTICLE INFO

Article history:
Received 27 March 2014
Received in revised form
30 July 2014
Accepted 9 August 2014
Available online

Keywords:
Three dimensional integrated circuits (3D ICs)
Analytical modeling
Thermal conduction
Floorplanning

ABSTRACT

3D integrated circuits (3-D ICs) technology is a promising approach for next-generation semiconductor microelectronics. A 3D IC is formed by vertical interconnection of multiple substrates containing active devices which offer reduced die footprint and interconnect length. Thermal management of a multi die stack is a significant research challenge, for which rapid temperature computation in a 3D IC is desirable. This manuscript presents a non-iterative heat transfer model for predicting the three-dimensional temperature field in a multi-die 3D IC. The non-iterative model is much faster and accurate in comparison to finite element simulation and recently presented iterative models for temperature computation. The analytical model is used to compute the temperature field of a 3D IC with a large number of die. The model is also used to examine the effect of various parameters on the computed temperature field. In particular, the effect of thermal contact resistance is presented. The model and results presented in this manuscript are expected be useful in rapid computation and effective thermal design of 3D ICs.
© 2014 Elsevier Masson SAS. All rights reserved.

1. Introduction

3D integrated circuits (3-D ICs) technology is a promising approach for next-generation semiconductor microelectronics [1–3]. A 3D IC is formed by vertical interconnection of multiple substrates containing active devices [4]. 3D ICs offer reduced die footprint and interconnect length without requiring dimensional scaling of transistors [5]. As a result, 3D ICs may result in similar performance benefits as dimensional scaling without the associated cost. One of the main technological challenges in 3D IC technology is in thermal management of a multi-die stack, and particularly in providing cooling to various substrates in the stack [5]. While one side of a traditional 2D IC on a single substrate is typically available for heat removal, there is an inherent lack of direct contact with a heat sink for device layers in the middle of the stack. Utilization of through-substrate vias (TSVs) for cooling has been investigated widely [6,7]. A number of microfluidics based approaches have been suggested for addressing this challenge [8–14].

An associated challenge in understanding and addressing thermal management in 3D ICs is to accurately and rapidly compute temperature fields in a 3D IC. This capability is important not only for cooling the 3D IC, but also to ensure optimal electrical performance. For example, the capability to predict peak temperature on each die in a 3D IC may be utilize to make smart decisions about load balancing and reallocation and maximize electrical performance of the stack [15]. Towards this, a 1D resistance network based thermal model has been proposed [16]. While this model highlighted important thermal phenomena that occur in 3D IC, its one-dimensional nature does not account for the non-uniform nature of heating on the surface of each die. Thermal network analysis for thermal design of the chip has been proposed and the effect of the area ratio of the interconnection in the interconnection layer on the maximum temperature is investigated. It also has been shown that in thermal network method the computational time is shorter than CFD method and it is very useful in parametric studies [17]. Thermal analysis of a typical 3D stack has been carried out using finite element simulations [18]. While numerical computations provide reasonable results, they have several disadvantages. Finite-element simulations are typically difficult to interface with traditional electrical design and analysis codes.

Heat transfer in a multi-layer structure with heating on top has been analyzed [19,20]. An iterative three-dimensional heat transfer models with non-uniform heating on the transistor plane of each die for 3D ICs has been developed [21]. Temperature distribution in a 3D ICs with unequally-sized die has also been determined [22]. Steady-state and transient temperature fields based on Fourier

* Corresponding author. 500 W First St, Rm 211, Arlington, TX 76019, USA. Tel.: +1 (817) 272 9338; fax: +1 (817) 272 2952.
E-mail address: jaina@uta.edu (A. Jain).

http://dx.doi.org/10.1016/j.ijthermalsci.2014.08.012
1290-0729/© 2014 Elsevier Masson SAS. All rights reserved.

series expansion and Laplace transforms respectively were studied. These models solve the underlying energy conservation equations in each die in an iterative fashion by assuming a distribution for the heat transfer $Q_i(x,y)$ from one die to the adjacent die. The temperature distribution is then determined using a solution of the governing energy conservation equation. Heat flow from one die to another is then computed, and used to improve the assumed heat flow distribution until convergence. The analytical nature of these models contributes towards a fundamental understanding of the heat transfer problem. For example, the dependence of various parameters on the temperature distribution can be easily studied. However, the iterative nature of these models increases computation speed. It is clearly desirable to develop a non-iterative analytical model for computing the temperature field in a 3D IC [21]. A non-iterative model will interface more seamlessly with electrical design tools, providing the capability of rapid temperature prediction. This capability would be valuable for both run-time performance management, as well as for pre-Silicon thermal design of the 3D IC.

This manuscript presents a non-iterative, analytical heat transfer model for computing three-dimensional temperature fields in a 3D IC. The governing energy equations with appropriate boundary conditions for N-die stack with different values of N are solved by first writing the solution in terms of infinite series, followed by deriving and solving ordinary differential equations for the coefficients in the series. Steady-state temperature fields predicted by this model compare well with FEM-based simulation results and previously developed iterative models. In addition, temperature computation based on the proposed models is much faster than numerical simulations or iterative approach. Section 2 describes the basic problem being addressed here, and outlines the solution methodology. Expressions for the temperature field are derived for perfect contact between layers (Section 2.1) as well as for non-zero thermal resistance between layers (Section 2.2). Accounting for non-zero thermal contact resistance is important, since such contact resistance is expected to exist between adjacent die in a 3D IC, and has been experimentally measured [23–25]. Results from this model are compared with previous papers for both accuracy and computation time. Several applications of the model are discussed in Section 3. These include temperature computation for a 3D IC with a large number of strata, as well as the effect of inter-die thermal contact resistance. Results discussed in this paper may find applications in development of tools for rapid thermal computation for 3D ICs.

2. Steady-state thermal conduction in a multi-die 3D IC

Fig. 1 shows a schematic of of the N-die stack under consideration, and top view of one of the die. The die stack consists of N die, each die is a cuboid of size a by b by c_i. Thermal conductivity k of each die is assumed to be isotropic and temperature-independent. A heat spreader and/or heat sink is assumed to be attached to the bottom-most die. The effect of the heat spreader/sink is modeled using a convective heat transfer coefficient h on the bottom surface of the bottom-most die. The top surface of the die stack, which is typically attached to the electronic package is assumed to be adiabatic, since the thermal resistance of the electronic package is typically much larger than the heat spreader/sink. All side surfaces are assumed to be adiabatic. Spatially-varying heating $Q_i(x,y)$ is assumed to occur on the top surface of each die. The primary interest is in developing a model for rapidly computing the temperature fields $T_i(x,y,z)$.

In this case, the governing energy conservation equation is

$$\frac{\partial^2 T_i}{\partial x^2}+\frac{\partial^2 T_i}{\partial y^2}+\frac{\partial^2 T_i}{\partial z^2}=0 \tag{1}$$

Subject to boundary conditions

$$\frac{\partial T_i}{\partial x}=0 \quad \text{at} \quad x=0,a \tag{2}$$

$$\frac{\partial T_i}{\partial y}=0 \quad \text{at} \quad y=0,b \tag{3}$$

Boundary conditions in the z direction include heat flux condition at the top of the Nth die, and convective boundary condition at the bottom of the first die.

$$\frac{\partial T_1}{\partial z}=\frac{h}{k}T_1 \quad \text{at} \quad z=0 \tag{4}$$

$$\frac{\partial T_N}{\partial z}=\frac{1}{k}Q_N(x,y) \quad \text{at} \quad z=c_N \tag{5}$$

In addition, continuity of temperature and conservation of heat flux at the interfaces between adjacent die provide additional boundary conditions. Two specific cases are considered in the following sub-sections, one with perfect thermal contact between adjacent die, and one with a given thermal contact resistance between adjacent die.

2.1. Perfect thermal contact

In case of perfect thermal contact between adjacent die, the temperature of the two die at the interface must be equal.

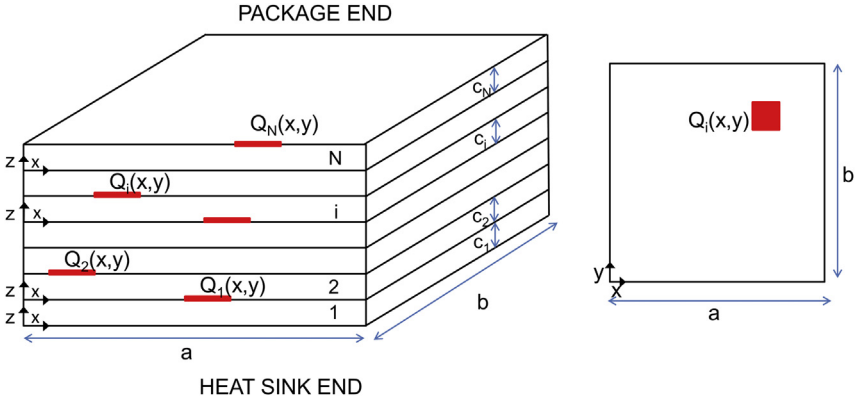

Fig. 1. Schematic of the N-die stack, and a cross-section view of the ith die showing the production of heat on the top surface.

$$T_{i+1}|_{z=0} = T_i|_{z=c_i} \quad i = 1, \ldots, N-1 \tag{6}$$

Further, energy conservation at the interface yields

$$k\frac{\partial T_i}{\partial z}\bigg|_{z=c_i} = Q_i(x,y) + k\frac{\partial T_{i+1}}{\partial z}\bigg|_{z=0} \quad i = 1, \ldots, N-1 \tag{7}$$

The governing equation represented by Equations (1)–(7) is solved using Fourier cosine series expansion in the homogeneous x and y directions [26]. Similar to the approach outlined in a previous paper [21,22], the solution for the temperature field $T_i(x,y,z)$ is written as:

$$T_i(x,y,z) = a_{i,0}(z) + \sum_{m=0}^{\infty}\sum_{n=0}^{\infty} a_{i,nm}(z)\cos\left(\frac{n\pi x}{a}\right)\cos\left(\frac{m\pi y}{b}\right) \tag{8}$$

This section presents an analytical approach to derive explicit expressions for the z-dependent coefficients $a_{i,0}(z)$ and $a_{i,nm}(z)$ that eliminates the need for iterative determination of the temperature fields using temperature and heat flux matching at the interfaces, as recently discussed [21,22]. To do so, the Fourier cosine series expansions of $Q_i(x,y)$ are first written as follows

$$Q_i(x,y) = b_{i,0} + \sum_{m=0}^{\infty}\sum_{n=0}^{\infty} b_{i,nm}\cos\left(\frac{n\pi x}{a}\right)\cos\left(\frac{m\pi y}{b}\right) \tag{9}$$

where the coefficients $b_{i,0}$ and $b_{i,nm}$ may be determined as

$$b_{i,0} = \frac{1}{ab}\int_0^b\int_0^a Q_i(x,y)\mathrm{d}x\mathrm{d}y \tag{10}$$

$$b_{i,nm} = \frac{\delta_{nm}}{ab}\int_0^b\int_0^a Q_i(x,y)\cos\left(\frac{n\pi x}{a}\right)\cos\left(\frac{m\pi y}{b}\right)\mathrm{d}x\mathrm{d}y \tag{11}$$

where δ_{nm} is 0 if n and m are both zero, 4 if n and m are both non-zero, and 2 otherwise.

To determine $a_{i,0}(z)$ and $a_{i,nm}(z)$, the temperature field given in Equation (8) is first substituted in the governing energy Equation (1), which results in ordinary differential equations in $a_{i,0}(z)$ and $a_{i,nm}(z)$. The solution is found to be

$$a_{i,0}(z) = A_{i,0} + B_{i,0}z \tag{12}$$

$$a_{i,nm}(z) = A_{i,nm}\exp(\gamma_{nm}z) + B_{i,nm}\exp(-\gamma_{nm}z) \tag{13}$$

where $\gamma_{nm} = \sqrt{(n\pi/a)^2 + (m\pi/b)^2}$.

The coefficients in Equation (12) are determined by applying the boundary conditions in z direction, Equations (4)–(7), resulting in a set of $2N$ equations in $2N$ variables, i.e. $A_{i,0}$ and $B_{i,0}$, where $i = 1, 2, \ldots, N$. By careful rearrangement of terms, an explicit analytical solution is derived to be

$$B_{i,0} = \sum_{i^*=i}^{N}\frac{b_{i^*,0}}{k} \quad i = 1, \ldots, N \tag{14}$$

$$A_{i,0} = \frac{1}{h}\sum_{i^*=1}^{N} b_{i^*,0} + \sum_{i^*=1}^{i-1}\left[c_{i^*}\sum_{j=i^*}^{N}\frac{b_{j,0}}{k}\right] \quad i = 1, \ldots, N \tag{15}$$

Similarly, an analytical solution for $A_{i,nm}$ and $B_{i,nm}$ is found by inserting the expression for $a_{i,nm}$ given by Equation (13) into the z boundary conditions. This results in

$$A_{i,nm} = \frac{\left(\frac{b_{N,nm}}{k\lambda_{nm}}\right) + \sum_{i^*=1}^{N-1}\left[r_{i^*,nm}\exp\left(\gamma_{nm}\sum_{j=i^*+1}^{N}c_j\right)\right] + \sum_{i^*=1}^{N-1}\left[r_{i^*,nm}\exp\left(-\gamma_{nm}\sum_{j=i^*+1}^{N}c_j\right)\right]}{\exp\left(\gamma_{nm}\sum_{i^*=1}^{N}c_{i^*}\right) - P_{nm}\exp\left(-\gamma_{nm}\sum_{i^*=1}^{N}c_{i^*}\right)}\exp\left(\gamma_{nm}\sum_{i^*=1}^{i-1}c_{i^*}\right)$$
$$-\sum_{i^*=1}^{i-1} r_{i^*,nm}\exp\left[\gamma_{nm}\sum_{j=i^*+1}^{i-1}c_j\right] \quad i = 1, \ldots, N \tag{16}$$

$$B_{i,nm} = \frac{\left(\frac{b_{N,nm}}{k\lambda_{nm}}\right) + \sum_{i^*=1}^{N-1}\left[r_{i^*,nm}\exp\left(\gamma_{nm}\sum_{j=i^*+1}^{N}c_j\right)\right] + \sum_{i^*=1}^{N-1}\left[r_{i^*,nm}\exp\left(-\gamma_{nm}\sum_{j=i^*+1}^{N}c_j\right)\right]}{\exp\left(\gamma_{nm}\sum_{i^*=1}^{N}c_{i^*}\right) - P_{nm}\exp\left(-\gamma_{nm}\sum_{i^*=1}^{N}c_{i^*}\right)}P_{nm}\exp\left(-\gamma_{nm}\sum_{i^*=1}^{i-1}c_{i^*}\right)$$
$$+\sum_{i^*=1}^{i-1} r_{i^*,nm}\exp\left[-\gamma_{nm}\sum_{j=i^*+1}^{i-1}c_j\right] \quad i = 1, \ldots, N \tag{17}$$

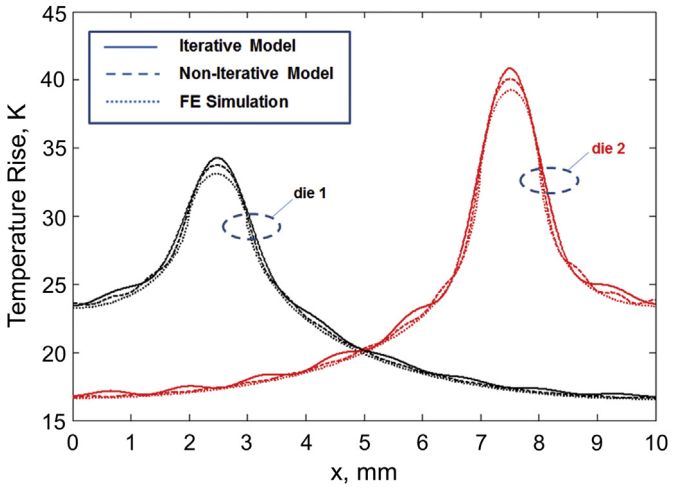

Fig. 2. Comparison of temperature determined from the non-iterative model with iterative and finite-element simulation results along the cross-section lines in the middle of every hotspot.

where

$$r_{i,nm} = \frac{b_{i,nm}}{2k\gamma_{nm}} \quad i = 1, \ldots, N-1 \tag{18}$$

$$P_{nm} = \frac{k\gamma_{nm} - h}{k\gamma_{nm} + h} \tag{19}$$

The treatment above assumes that each die has the same thermal conductivity, which is likely, since 3D integration so far is based on bonding die of the same material with each other to form the die stack. However, in case of integration with die of dis-similar materials, the equations above can be easily re-derived considering each die to have a distinct thermal conductivity, k_i. In this case, a set of linear equations for coefficients $A_{i,nm}$ and $B_{i,nm}$ can still be derived. However, these equations do not admit a straight-forward, explicit solution, and must instead be solved using techniques such as matrix inversion.

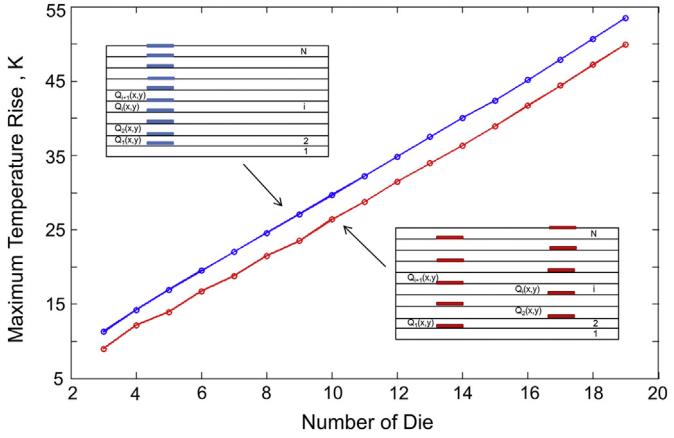

Fig. 3. Maximum temperature rise in N-die stack as a function of number of die for two different cases.

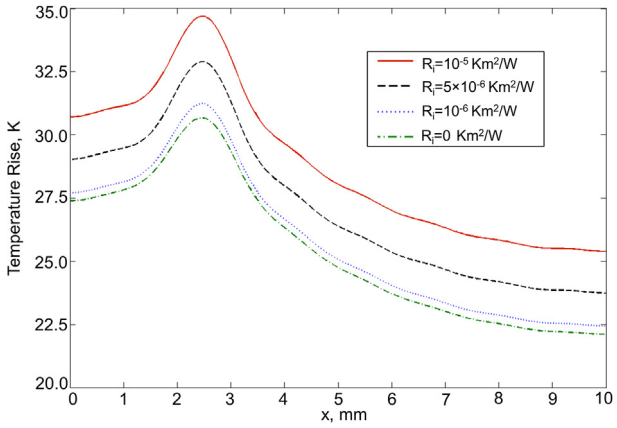

Fig. 4. Temperature rise at top surface of die 5 for a ten-die stack case with different values of thermal contact resistance.

2.2. Non-zero thermal contact resistance between interfaces

This sub-section considers the case where a non-zero thermal contact resistance R_i exists between the ith and $(i+1)$th die. In such a case, continuity at interfaces, described previously by Equation (6) is modified to the following:

$$T_{i+1}|_{z=0} = T_i|_{z=c_i} + kR_i \left.\frac{\partial T_{i+1}}{\partial z}\right|_{z=0} \quad \text{for} \quad i = 1, \ldots, N-1 \tag{20}$$

Similar to the perfect thermal contact presented in Section 2.1, the temperature solution for this case is still governed by Equation (8), with expressions for coefficients given by Equations (12) and (13). In a manner similar to Section 2.1, explicit expressions for coefficients $A_{i,0}$, $B_{i,0}$ are derived to be

$$B_{i,0} = \sum_{i^*=i}^{N} \frac{b_{i^*,0}}{k} \quad i = 1, \ldots, N \tag{21}$$

$$A_{i,0} = \frac{1}{h}\sum_{i^*=1}^{N} b_{0,i^*} + \sum_{i^*=1}^{i-1}\left[c_{i^*}\sum_{j=i^*}^{N}\frac{b_{0,j}}{k}\right] + \sum_{i^*=1}^{i-1}\left[kR_{i^*}\sum_{j=i^*+1}^{N}\frac{b_{0,j}}{k}\right] \quad i = 1, \ldots, N \tag{22}$$

Due to the added complexity in boundary condition Equation (20), the coefficients $A_{i,nm}$ and $B_{i,nm}$ in Equation (13) cannot be

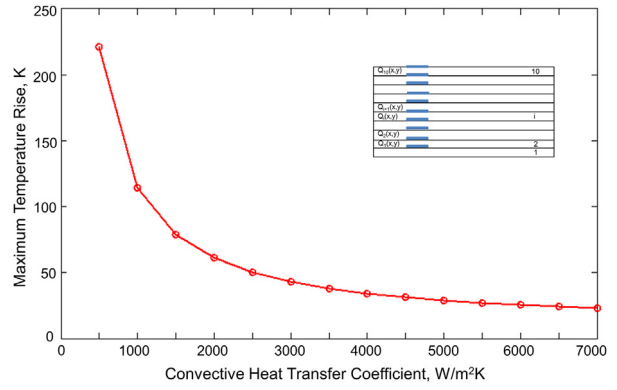

Fig. 5. Maximum temperature rise at top surface of die 5 in a ten-die stack case with different values of convective heat transfer coefficient.

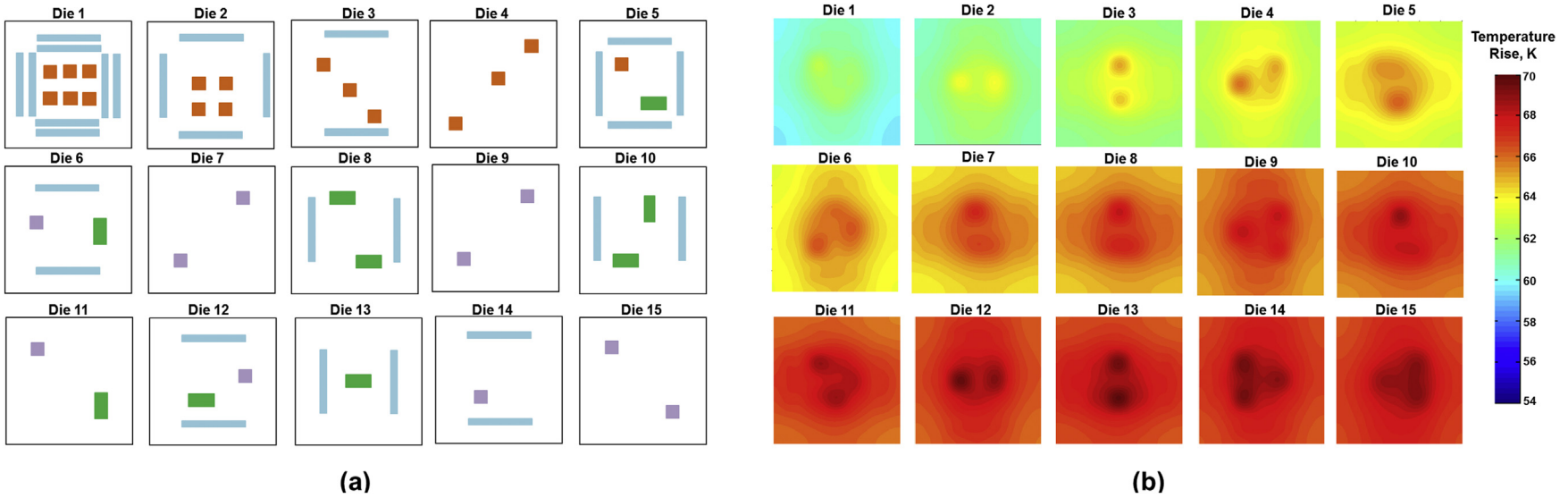

Fig. 6. (a) Power map of a 15-die stack representative of a APU–GPU microprocessor unit, (b) computed temperature field for the power map.

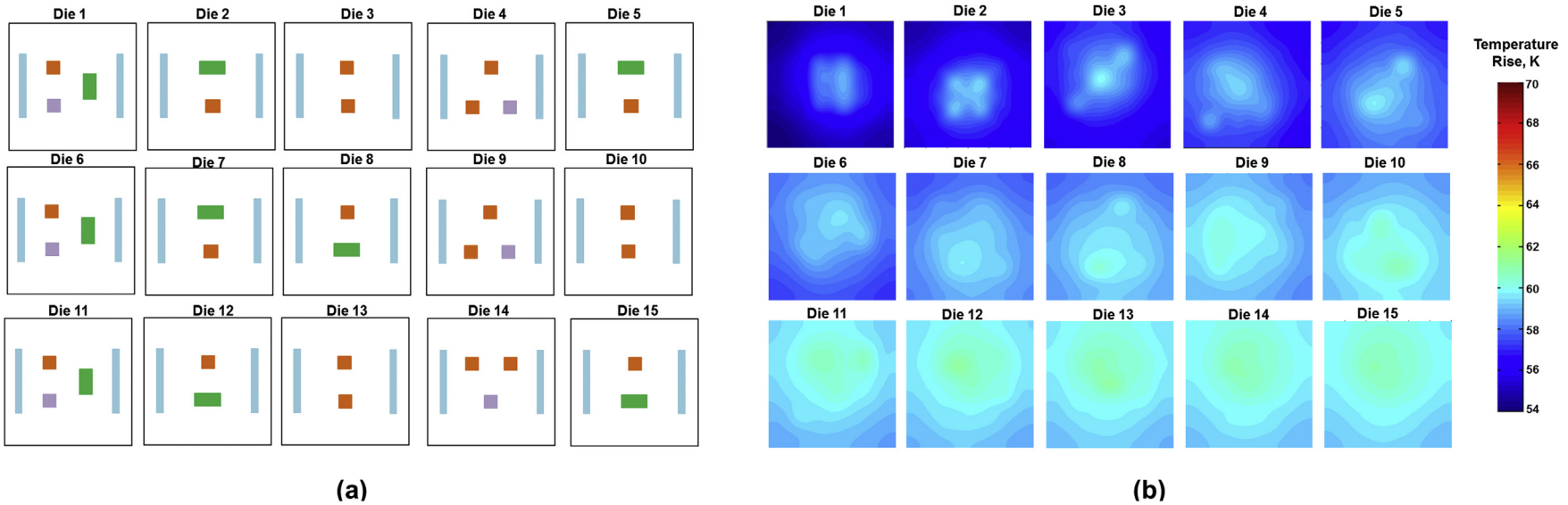

Fig. 7. (a) Power map of an alternative, thermally-friendly floorplan for the 15-die stack, (b) computed temperature field for the power map.

described explicitly. Instead, a set of $2N$ equations in $2N$ unknowns $A_{i,nm}$ and $B_{i,nm}$ are derived using the z boundary conditions. The equations are

$$\gamma_{nm}(A_{1,nm}-B_{1,nm}) = \frac{h}{k}(A_{1,nm}+B_{1,nm}) \tag{23}$$

$$k\gamma_{nm}(A_{N,nm}exp(\gamma_{nm}c_N) - B_{N,nm}\exp(-\gamma_{nm}c_N)) = b_{N,nm} \tag{24}$$

$$\begin{aligned} &A_{i+1,nm}(1-kR_i\gamma_{nm}) + B_{i+1,nm}(1+kR_i\gamma_{nm}) \\ &= A_{i,nm}\exp(\gamma_{nm}c_i) + B_{i,nm}\exp(-\gamma_{nm}c_i) \quad i=1,\ldots,N-1 \end{aligned} \tag{25}$$

$$\begin{aligned} A_{i+1,nm}-B_{i+1,nm} = A_{i,nm}\exp(\gamma_{nm}c_i) - B_{i,nm}\exp(-\gamma_{nm}c_i) \\ -\frac{b_{i,nm}}{k\gamma_{nm}} \quad i=1,\ldots,N-1 \end{aligned} \tag{26}$$

A solution of Equations (23)–(26) using commonly available techniques such as matrix inversion results in solutions for the coefficients $A_{i,nm}$ and $B_{i,nm}$. This completes the solution for non-zero thermal contact resistance between adjacent die.

3. Results and discussion

Based on the analytical method described in the previous section, the temperature field on a two-die stack is computed and compared with finite-element simulation results, and a previously reported iterative method [21]. It is found that using about 20 eigenvalues provides sufficient accuracy, and that further eigenvalues do not contribute significantly to the computed temperature value. Each die of size 10 mm by 10 mm is assumed to have a 5 W hotspot of size 1 mm by 1 mm, centered at (2.5 mm, 2.5 mm) for die1 and (7.5 mm, 7.5 mm) for die2 respectively. Heat dissipation is assumed to occur through a heat sink attached to die1. The heat sink is modeled using a convective heat transfer coefficient of 5000 W m^{-2} K^{-1}. A plot of temperature rise along a horizontal line passing through the hotspot centers is shown in Fig. 2. The temperature field computed using the model presented in Section 2.1 is in excellent agreement with finite-element simulations carried out in commercial software. The non-iterative model presented in this paper is found to be more accurate than the previously reported iterative model [21]. More importantly, the computation time for the non-iterative model is much lower than both finite-element simulations and the iterative model. This improvement is particularly significant when the number of die in the stack is larger than 10, making this model appropriate for rapid temperature computation for large, multi-die systems.

Fig. 3 plots the maximum temperature rise in the 3D IC as a function of number of die in the stack. While the model is capable of accounting for any general heat distribution, in this case, a single hotspot of size 1 mm by 1 mm and power 1.0 W is assumed to be present on each die. Two specific cases are considered – one in which the hotspots are vertically aligned with each other, and a second case in which the hotspots are alternatively staggered, as shown in Fig. 3. As expected, the temperature increases rapidly as the number of die in the stack increases. Further, the temperature rise in the first case, where the hotspots are aligned, is greater than the second case. This happens because of increased power density due to overlap of hotspots in the first case.

Depending on the nature of integration, some thermal contact resistance may exist between adjacent die in a 3D IC stack [23–25]. This thermal contact resistance may occur due to the presence of an underfill material around metal pillars that bond adjacent die together. In addition, a non-zero thermal contact resistance may also occur due to imperfect bonding between metal pads on adjacent die. Since thermal contact resistances are known to impact thermal characteristics of microsystems [27,28], it is important to carry out an evaluation of the effect of thermal contact resistance on the temperature field in a 3D IC stack. Fig. 4 shows the temperature curve along a line passing through the hotspot on die5 in a 10 die stack, where each die has an aligned, 1.0 W hotspot of size 1 mm by 1 mm. This curve is plotted for a number of thermal contact resistance values, computed using the model presented in Section 2.2. For comparison, the perfect thermal contact resistance model, presented in Section 2.1 is also plotted. Fig. 4 shows that, as expected, temperature rise increases as thermal contact resistance increases. This plot shows the importance of engineering the inter-die interface in order to reduce thermal contact resistance and hence reduce temperature rise.

Further, the effect of the convective boundary condition at the bottom-most die is investigated. Fig. 5 plots the peak temperature in a ten-die stack similar to the one considered in Fig. 3 as a function of convective heat transfer coefficient. It is found that the maximum temperature in the ten-die stack decreases rapidly when convective heat transfer coefficient increases. The temperature reduction is significant at low values of the convective heat transfer, but this effect diminishes somewhat as the heat transfer coefficient increases.

Finally, in order to demonstrate the capability of the analytical model, the temperature profile on each die for a 15-die case is computed for non-uniform heating, shown in Fig. 6(a). Each of the orange (in the web version), blue, green and gray blocks corresponds to a heat rate of 75.0, 20.0, 17.5 and 4.0 W/cm^2 respectively. The temperature field on each die is computed using the model presented in Section 2.1. The computed temperature fields are shown in Fig. 6(b) for each die. The temperature fields shown in Fig. 6(b) take into account non-uniform heating in different blocks as well as their in-plane and out-of-plane proximity. The computation time for the model for a 15 die stack is about 170 s, which is much faster than both finite-element simulations as well as iterative models for temperature computation [21].

The floorplan for the 15-die case considered in Fig. 6 is redistributed in order to obtain a more thermal friendly floorplan. It is expected that distributing the orange blocks – that generate the highest power density – more uniformly amongst all dies may result in a more uniform and lower temperature distribution. The resulting heating profile and computed temperature distribution on each die are shown in Fig. 7(a) and (b) respectively. Note that temperature distributions in Figs. 6(b) and 7(b) are both plotted in the same color range, for ease of comparison. As expected, the thermal friendly redistribution of heat generating blocks results in considerably reduced temperature and greater thermal uniformity. The redistribution of the floorplan carried out here is based on reducing power density by distributing the high power density blocks uniformly, the power map in Fig. 7(a) is not necessarily thermally optimal. Determination of a thermally optimal power map may require iterative redistribution with several steps. Further, floorplanning optimization is a multi-disciplinary process [29] that requires the optimization of several objectives related to thermal and electrical performance. It is expected that the analytical model presented in this paper may aid such a multidisciplinary floorplanning optimization process by computing the temperature distribution at each step.

4. Conclusions

In this paper a non-iterative analytical approach for computing three-dimensional temperature field in a 3D IC has been investigated. For different values of number of stacks in 3D IC, the governing energy equations with appropriate boundary conditions have been solved. The steady state temperature field predicted by the model compared well with finite element simulation and the iterative model which presented in the past. Furthermore the model is much faster than numerical model and iterative model. The temperature distribution for large number of die has been presented and the effect of inter-die thermal contact resistance investigated. Also several application of the work discussed and the results may be useful in design and fast thermal computation of 3D IC.

Acknowledgments

This material is based upon work supported by the National Science Foundation under Grant No. CBET-1236370.

References

[1] K. Banerjee, S.J. Souri, K.C. Saraswat, 3-D ICs: a novel chip design for improving deep submicron interconnect performance and systems-on-chip integration, Proc. IEEE 89 (5) (2001) 602–633.
[2] R. Patti, Three-dimensional integrated circuits and the future of system-on-chip designs, Proc. IEEE 94 (6) (2006) 1214–1224.
[3] G. Loh, Y. Xie, B. Black, Processor design in three-dimensional die-stacking technologies, IEEE Micro 27 (3) (2007) 31–48.
[4] A.W. Topol, D.C. La Tulipe, L. Shi, D.J. Frank, K. Bernstein, S.E. Steen, A. Kumar, G.U. Singco, A.M. Young, K.W. Guarini, M. Leong, Three-dimensional integrated circuits, IBM J. Res. Dev. 50 (4) (2006).
[5] J.F. Li, C.W. Wu, Is 3D integration an opportunity or just a hype?, in: 15th Asia and South Pacific Design Automation Conference (ASPDAC), Jan. 18–21, Taipei, 2010, pp. 541–543.
[6] B. Goplen, S.S. Sapatnekar, Placement of thermal vias in 3D ICs using various thermal objectives, IEEE Trans. Comput. Aided Des. Integr. Circuits Syst. 26 (4) (2006) 692–709.
[7] J. Cong, G. Luo, Y. Shi, Thermal-aware cell and through-silicon-via co-placement for 3D ICs, in: DAC'11, June 5–10, San Diego, California, USA, 2011.
[8] C.R. King, J. Zaveri, M.S. Bakir, J.D. Meindl, Electrical and fluidic C4 interconnections for inter-layer liquid cooling of 3D ICs, in: Proc. Electronics Components Technol. Conf., 2010.
[9] Y.J. Kim, Y.K. Joshi, A.G. Fedorov, Y.J. Lee, S.K. Lim, Thermal characterization of interlayer microfluidic cooling of three-dimensional integrated circuits with nonuniform heat flux, J. Heat Transfer 132 (4) (2010) 041009.
[10] T. Brunschwiler, B. Michel, H. Rothuizen, U. Kloter, B. Wunderle, H. Oppermann, H. Reichl, Interlayer cooling potential in vertically integrated packages, Microsyst. Technol. 15 (1) (2009) 57–74.
[11] Y. Wei, Y. Joshi, Stacked micro channel heat sinks for liquid cooling of microelectronic components, ASME J. Electron. Packag. 126 (2004) 60–66.
[12] N. Khan, L.H. Yu, T.S. Pin, S.W. Ho, N. Su, W.Y. Hnin, V. Kripesh, D. Pinjala, J.H. Lau, T. Chuan, 3D packaging with through silicon via (TSV) for electrical and fluidic interconnections, in: Proceedings of 59th Electronics Components and Technology Conference, May 26–29, San Diego, 2009.
[13] T. Brunschwiler, B. Michel, H. Rothuizen, U. Kloter, B. Wunderle, H. Oppermann, H. Reichl, Forced convective interlayer cooling in vertically integrated packages, in: Proceedings of 11th Intersociety Conference on Thermal and Thermo Mechanical Phenomena in Electronic Systems (ITHERM), May 28–31, Orlando, Florida, 2008, pp. 1114–1125.
[14] S.P. Tan, K.C. Toh, N. Khan, D. Pinjala, V. Kripesh, Development of single phase liquid cooling solution for 3-D silicon modules, IEEE Trans. Compon. Packag. Manuf. Technol. 1 (4) (2011) 536–544.
[15] B. Goplen, S. Sapatnekar, Efficient thermal placement of standard cells in 3D ICs using a force directed approach, in: International Conference on Computer Aided Design, 2003, pp. 86–89.
[16] A. Jain, R.E. Jones, R. Chatterjee, S. Pozder, Analytical and numerical modeling of the thermal performance of three-dimensional integrated circuits, IEEE Trans. Compon. Packag. Technol. 33 (1) (2010) 56–63.
[17] T. Hatakeyama, M. Ishizuka, S. Nakagawa, Estimation of maximum temperature in 3D-integrated package by thermal network method, in: Proceedings of 12th Electronics Packaging Technology Conference, Dec. 8–10, 2010, pp. 68–71.
[18] C. Torregiani, B. Vandevelde, H. Oprins, E. Beyne, I.D. Wolf, Thermal analysis of hot spots in advanced 3D stacked structures, in: Proceedings of 15th International Workshop on Thermal Investigations of ICs and Systems (THERMINIC), Oct. 7–9, Leuven, Belgium, 2009, pp. 56–60.
[19] A. Haji-Sheikh, J.V. Beck, Temperature solution in multi-dimensional multilayer bodies, Int. J. Heat Mass Transfer 45 (2002) 1865–1877.
[20] J. Geer, A. Desai, B. Sammakia, Heat conduction in multilayered rectangular domains, ASME J. Electron. Packag. 129 (2007) 440–451.
[21] L. Choobineh, A. Jain, Analytical solution for steady-state and transient temperature field in vertically integrated three-dimensional integrated circuits (3D ICs), IEEE Trans. Compon. Packag. Technol. 2 (12) (2012) 2031–2039.
[22] L. Choobineh, A. Jain, Determination of temperature distribution in three-dimensional integrated circuits (3D ICs) with unequally-sized die, Appl. Therm. Eng. 56 (1) (2013) 176–184.
[23] H. Oprins, V. Cherman, K. Rebibis, K. Vermeersch, C. Gerets, B. Vandevelde, A. La Manna, G. Beyer, E. Beyne, Transient analysis based thermal characterization of die-die interfaces in 3D-ICs, in: Proceedings of IEEE ITherm, San Diego, CA, 2012, pp. 1395–1404.
[24] K. Matsumoto, S. Ibaraki, K. Sueoka, K. Sakuma, H. Kikuchi, Y. Orii, F. Yamada, Experimental thermal resistance evaluation of a three-dimensional (3D) chip stack, in: Proceedings of IEEE SEMI-THERM, San Jose, CA, 2011.
[25] E.G. Colgan, P. Andra, B. Dang, J.H. Magerlein, J. Maria, R.J. Polastre, Measurement of microbump thermal resistance in 3D chip stacks, in: Proceedings of IEEE SEMI-THERM, San Jose, CA, 2012.
[26] M.N. Özişik, Boundary Value Problems of Heat Conduction, first ed., Dover Publications, 1989.
[27] E. Bozorg-Grayeli, J.P. Reifenberg, M. Asheghi, H.S.P. Wong, K.E. Goodson, Thermal transport in phase change memory materials, Annu. Rev. Heat Transfer 16 (2013) 397–428.
[28] M. Yovanovich, Four decades of research on thermal contact, gap, and joint resistance in microelectronics, IEEE Trans. Compon. Packag. Technol. 28 (2) (2005) 182–206.
[29] A. Jain, S.M. Alam, S. Pozder, R.E. Jones, Thermal–electrical co-optimization of floor planning of three-dimensional integrated circuits under manufacturing and physical design constraints, IET Comput. Digital Tech. 5 (3) (2011) 169–178.